A Molecular Dynamics Study of the Bis-Intercalation Complexes of Echinomycin with d(ACGT)$_2$ and d(TCGA)$_2$: Rationale for Sequence-Specific Hoogsteen Base Pairing

José Gallego, Angel R. Ortiz,† and Federico Gago*

Departamento de Fisiología y Farmacología, Universidad de Alcalá de Henares, 28871 Madrid, Spain

Received November 9, 1992

The behavior of the complexes of echinomycin with the DNA tetramers d(ACGT)$_2$ and d(TCGA)$_2$, in which the terminal AT base pairs are in either a Hoogsteen or a Watson–Crick conformation, has been explored by molecular dynamics taking into account experimental data from NMR studies (Gao and Patel. *Biochemistry* **1988**, *27*, 1744–1751). The DNA binding specificity of echinomycin appears to be the result of a subtle balance between stabilizing and destabilizing forces. Among the former is a number of hydrogen bonds between the alanine residues of echinomycin and both the N3 and 2-amino groups of the guanine bases which decisively determine the strong affinity of the antibiotic for CpG steps. On the other hand, there appears to be an unfavorable dipolar interaction between the chromophores of the antibiotic and the CpG step. This electrostatic component of the stacking interactions also contributes to explaining the conformational preferences of the flanking sequences: upon Hoogsteen pairing, the dipole moment of an AT base pair is found to increase significantly and alter its relative orientation. In the d(ACGT)$_2$:echinomycin complex, this arrangement helps to improve the stacking interactions with the quinoxaline-2-carboxamide system, but would lead to unfavorable dipolar interactions in the d(TCGA)$_2$ complex. The bearing of these findings on the binding of echinomycin to several sequences as well as on the altered binding selectivity of other members of the quinoxaline family of antibiotics is also discussed.

Introduction

The DNA molecule is the primary target of many antitumor agents. Among the binding modes of drugs to DNA, both intercalative and nonintercalative mechanisms have been described, and in both cases a certain degree of sequence selectivity has been shown. Interestingly, minor groove binders show a tendency to bind to AT-rich DNA better than to GC-containing sequences whereas most intercalators get sandwiched at GpC or CpG steps,[1] with the notable exception of TANDEM, which also prefers AT runs.[2] In addition to the experimental approach, modeling studies have proved of value in order to understand the determinants of specificity involved in the recognition process[3] and can help in the design of new compounds with tailor-made binding properties.

Echinomycin is one of several antibiotics produced by *Streptomyces echinatus* that consists of two quinoxaline chromophores attached to a cyclic octadepsipeptide ring with a thioacetal cross-bridge (Figure 1). It displays potent cytotoxic activity that is generally accepted to arise from its capacity to bind to cellular DNA as a bis-intercalator, as shown in a wide range of viscosimetric, X-ray, and NMR studies.[4] Echinomycin is currently in phase II clinical trials as an antitumor agent.[5]

Footprinting experiments with DNase I[6] and chemical probes[7] have demonstrated that echinomycin binds specifically to CpG sequences and shows some preference for AT as the flanking base pairs.

X-ray crystal structures are available for the complexes of echinomycin with the d(CGTACG)$_2$ hexamer[8] and of the closely related analogue triostin A with d(CGTACG)$_2$[9] and d(GCGTACGC)$_2$.[10] A number of NMR studies have also been undertaken with echinomycin bound to different

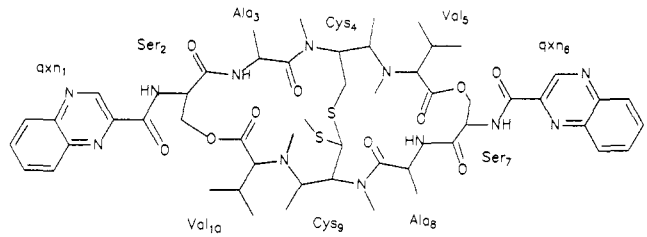

Figure 1. Chemical structure of echinomycin. Echinomycin is one member of the quinoxaline family of antibiotics, which are characterized by a cross-linked octadepsipeptide ring bearing two quinoxaline chromophores (qxn). In the echinomycin analogue triostin A, a disulfide bond replaces the thioacetal cross-link.

DNA oligomers: d(ACGT)$_2$ and d(TCGA)$_2$,[11] d(GCGC)$_2$, d(CCGG)$_2$, and d(AAACGTTT)$_2$,[12] d(ACGTACGT)$_2$ and d(TCGATCGA)$_2$,[13] and d(ACGTATACGT)$_2$.[14] This experimental work has provided considerable insight into the structural features of these complexes. Most notably, it has shown that in every complex studied the quinoxaline rings of the antibiotic intercalate on both sides of the CpG steps and that three major factors contribute to stabilizing the echinomycin–DNA complexes: (1) van der Waals interactions between the peptide part of the antibiotic and the minor grooves of the oligomers, (2) stacking interactions between the quinoxaline rings and the adjacent base pairs, and (3) several hydrogen bonds between the NH and carbonyl groups of alanines and the N3 and 2-amino groups of guanines, respectively. These hydrogen bonds are widely considered to be crucial for the binding specificity of echinomycin to CpG steps.[5]

The conformation of echinomycin complexed with DNA is similar to that found for the isolated antibiotic in solution.[15,16] In contrast, the DNA oligomers undergo drastic conformational changes upon binding of the drug. Most important among such changes are the unwinding of the double helices and the induction of a Hoogsteen

* Author to whom correspondence should be addressed.
† Present address: European Molecular Biology Laboratory, Meyerhofstrasse 1, Postfach 10.2209, D-6.900 Heidelberg, Germany.

0022-2623/93/1836-1548$04.00/0

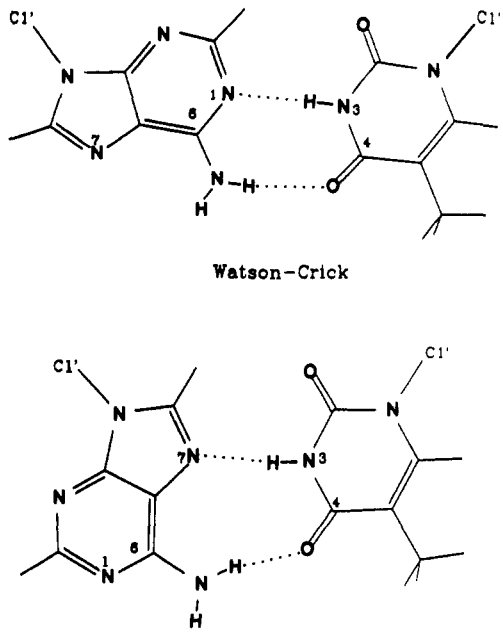

Figure 2. Hoogsteen and Watson–Crick pairing arrangements in an AT base pair. Note that the number of hydrogen bonds is the same in both conformations.

hydrogen bonding scheme in the base pairs adjacent to the CpG binding sites. In order for a Hoogsteen base pair to form, the purine base must rotate 180° about the glycosidic bond thus adopting a syn orientation relative to the sugar (Figure 2). This base-pairing rearrangement is sequence-dependent, since it only appears when the purine base is located on the 5′ side of the CpG binding steps: it is detected in d(ACGT)$_2$, d(GCGC)$_2$, d(CGTACG)$_2$, d(ACGTACGT)$_2$, d(ACGTATACGT)$_2$, and d(GCGTACGC)$_2$, but not in d(TCGA)$_2$, d(CCGG)$_2$, d(AAACGTTT)$_2$, and d(TCGATCGA)$_2$. In the sequences where the aforementioned condition is fulfilled, Hoogsteen pairing is always detected in the *terminal* base pairs, both in the crystalline state and in solution. The *internal* base pairs separating two CpG binding sites are also Hoogsteen paired in the solid state but seem to alternate between Hoogsteen and either an open or a Watson–Crick paired state in solution, as reported for the d(ACGTACGT)$_2$:(echinomycin)$_2$ complex.[13] Hoogsteen base pairing is not clearly detected in solution for the internal base pairs if the CpG binding sites are separated by more than two base pairs, as in the d(ACGTATACGT)$_2$:(echinomycin)$_2$ complex.[14] If there is only one CpG binding step, the internal base pairs adjacent to it remain Watson–Crick paired, as is the case in the d(AAACGTTT)$_2$:echinomycin complex.[12]

In their NMR studies of DNA oligomers with two echinomycin binding sites, Gilbert and Feigon have found cooperative binding only to the sequences where Hoogsteen pairs appear, i.e. to d(ACGTACG)$_2$ and d(ACGTATACGT)$_2$, but not to d(TCGATCGA)$_2$.[13,14] The binding constant for echinomycin binding to d(ACGTACGT)$_2$ was also found to be higher than that for binding to the nonalternating purine–pyrimidine sequence, d(TCGATCGA)$_2$.[13] Other studies have shown that the bisquinoline analogue of echinomycin favors binding to d(ACGT)$_2$, a sequence where the AT pairs adopt a Hoogsteen scheme, over d(TCGA)$_2$, in which all the bases remain Watson–Crick paired.[17]

In the present study,[18] we undertake a theoretical investigation of the factors that determine the conformational preferences of the flanking base pairs on both sides of the CpG binding step. An early computational study focused on the relative stability of the d(CGTACG)$_2$:(triostin A)$_2$ complex with the central AT base pairs in either Hoogsteen or Watson–Crick pairing,[19] but did not consider the alternative central sequence, i.e. d(CGATCG)$_2$. For their greater simplicity, we have chosen to study the complexes between echinomycin and the DNA tetramers d(ACGT)$_2$ and d(TCGA)$_2$, for which there is also conformational information from NMR spectroscopy.[11] Our research has addressed two main issues: (1) why the terminal base pairs in the d(ACGT)$_2$ complex are Hoogsteen paired while those in the d(TCGA)$_2$ one are not, and (2) why the former complex is more stable than the latter. By means of molecular dynamics simulations in aqueous solution, we have analyzed the behavior of the four possible systems: d(ACGT)$_2$:echinomycin and d(TCGA)$_2$:echinomycin with both terminal AT base pairs in either Hoogsteen (named A(h) and T(h), respectively) or Watson–Crick conformation (A(w) and T(w)) (Figure 3).

Results and Discussion

Both the total potential energy of the systems and the root-mean-square deviation of the complexes with respect to the initial structures remain stable along the simulation time (Figure 4). The progression of these two parameters indicates that the DNA:echinomycin complexes do not experience large conformational changes during the sampling time and thus can be considered to be in a state near equilibrium. Since the movement of the counterions has a profound influence on the behavior of highly charged molecules like DNA, the diffusion constant of the sodium ions in the four simulations was calculated from their respective mean square displacements (Figure 5), using the relation:

$$6D = \lim_{t\to\infty} \frac{\mathrm{d}[\langle(\vec{r}(t) - \vec{r}(0))^2\rangle_t]}{\mathrm{d}t} \qquad (1)$$

where $\vec{r}(t)$ denotes the coordinates of the ion at time t and the broken brackets ($\langle\rangle_t$) indicate a time average. The average Na^+ diffusion constant for the four systems is 0.60×10^{-5} cm^2 s^{-1}. Previously reported experimental and theoretical diffusion constants are 0.91×10^{-5} and 1.0×10^{-5} cm^2 s^{-1}, respectively, for Na^+ in bulk water,[20] and $(0.0–5.0) \times 10^{-5}$ cm^2 s^{-1} for Na^+ around DNA.[21] The comparatively low diffusion constants found for the sodium ions in the four simulations suggest that the ions were effectively placed in minimum-energy configurations and validates the method used for their placement. Interestingly, the ion configurations seem to be more stable around the Watson–Crick complexes, for which much lower coefficients are found: 0.13 and 0.17 for A(w) and T(w) vs 1.20 and 0.94 for A(h) and T(h), respectively (Figure 5).

(a) General Structure of the Complexes. Stereoviews of the structures of the four systems can be seen in Figure 6. These conformations correspond to averages taken over the 30–40-ps period of the unrestrained simulations in aqueous solution, with bond and van der Waals distances optimized by means of a short-energy minimization. Comparison between these conformations and the corresponding water-minimized initial structures yields root-mean-square deviations of 1.77, 1.92, 1.22, and 1.27 Å for complexes A(h), A(w), T(h), and T(w), respec-

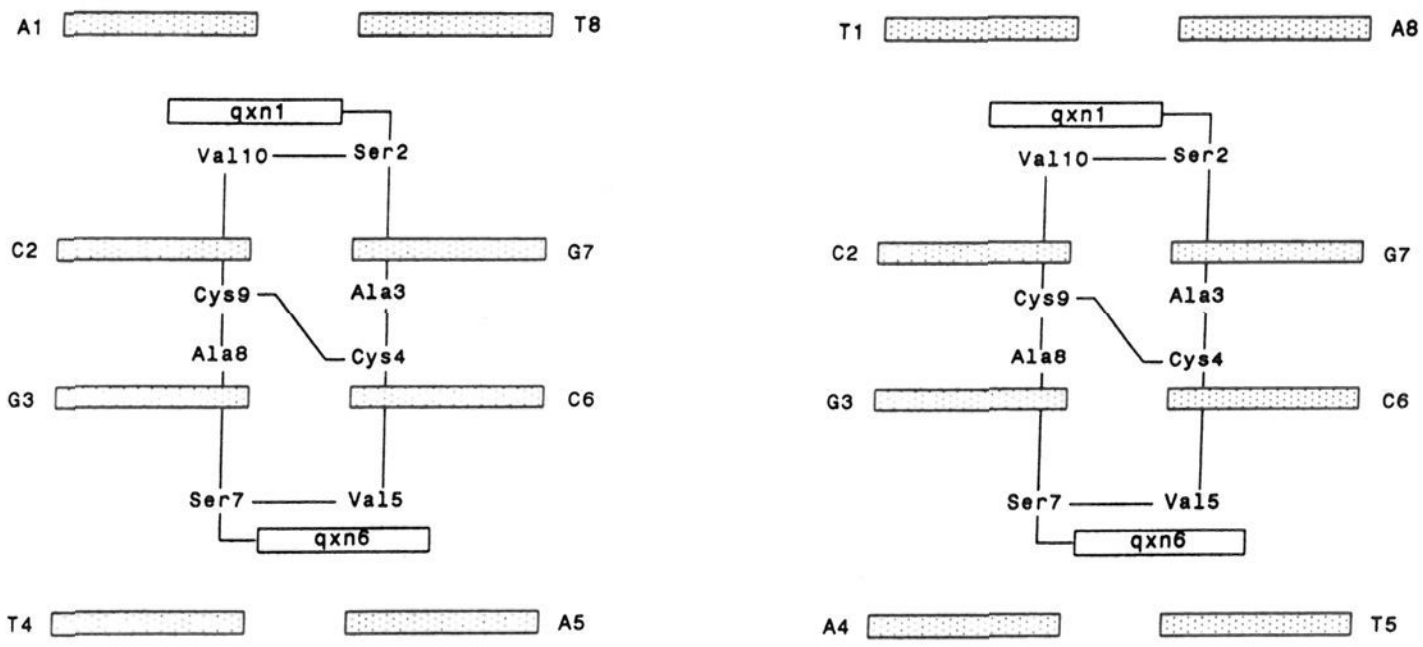

A T

Figure 3. Schematic views from the major groove of the complexes of echinomycin with $d(ACGT)_2$ and $d(TCGA)_2$, designated A and T, respectively. In each of them, the terminal AT pairs can display a Hoogsteen, A(h) and T(h), or a Watson–Crick, A(w) and T(w), hydrogen-bonding arrangement.

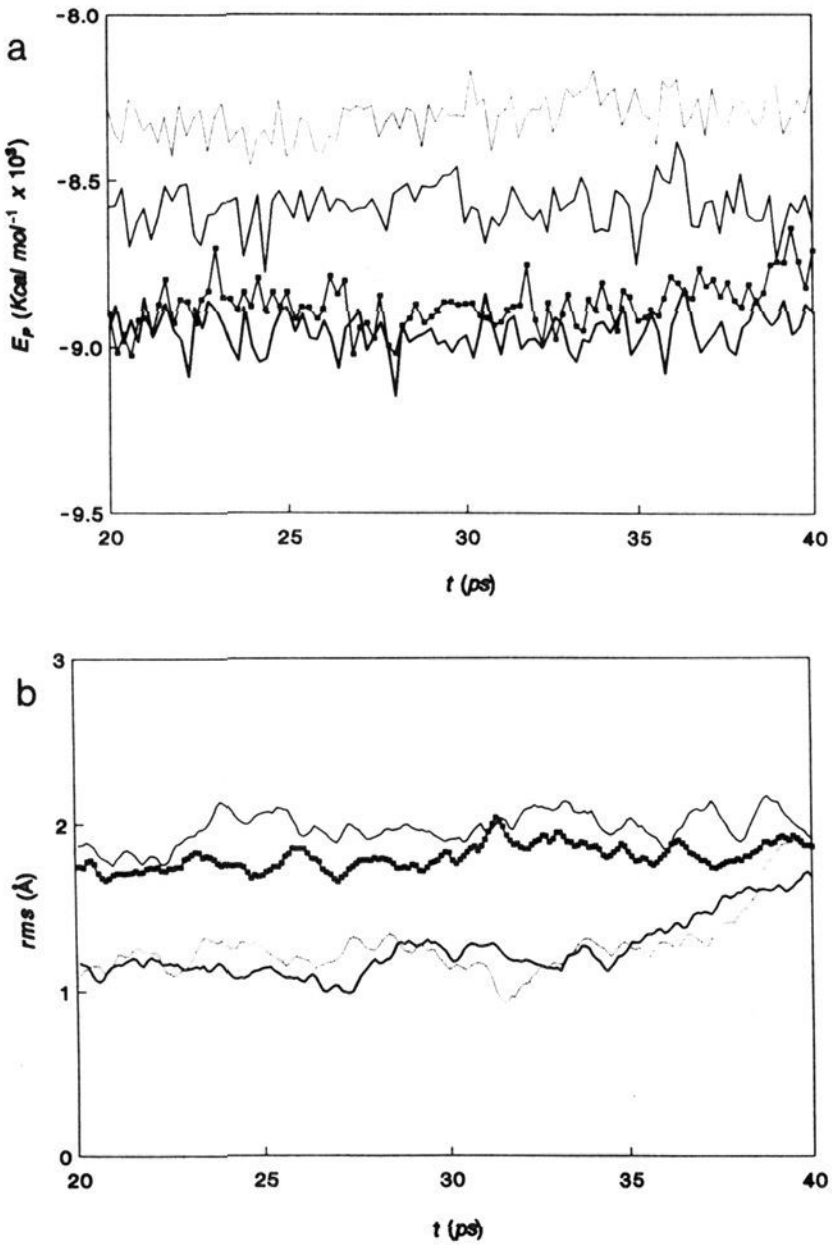

Figure 4. Total potential energies (a) and root-mean-square deviations from the initial structures (b) as a function of time of the four solvated DNA:echinomycin complexes during the sampling phase (20–40 ps): A(h) (□), A(w) (—), T(h) (···), and T(w) (—). The root-mean-square deviations were calculated using all non-hydrogen atoms of the complexes and superimposing the structures over the same atoms. The different values of potential energy are due to the different number of water molecules present in each of the systems.

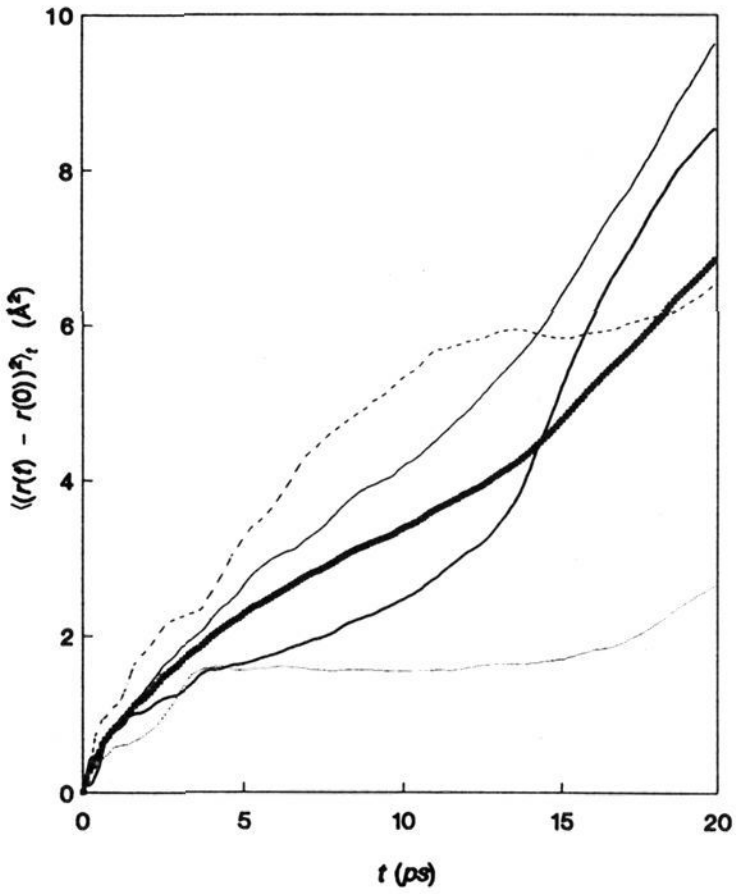

Figure 5. Mean square displacements of the sodium ions in the four simulations. The lines represent the average displacement of the six ions present in each system: A(h) (thick), A(w) (dashed), T(h) (thin), and T(w) (dotted). The line of squares is the average mean square displacement of all sodium ions in the four simulations.

tively. These values give another indication that the complexes did not undergo large conformational changes with respect to their initial structures during the simulations in water. The conformation of each pair of complexes with the same base pairing, i.e. A(h) and T(h), and A(w) and T(w), is similar, with root-mean-square deviations of 0.99 and 1.98 Å, respectively. The terminal DNA bases behave well in the sense that they remain paired even in the absence of hydrogen-bond constraints. The exceptions are bases A5 and T4 in the A(h) model, which are partially unpaired, and base T8 in the A(w) model, which goes out of plane (Figure 6). These deviations are due to end affects during the unrestrained dynamics simulations in water and could not be avoided despite extensive efforts aimed at the generation of more stable initial structures. The larger root-mean-square deviations

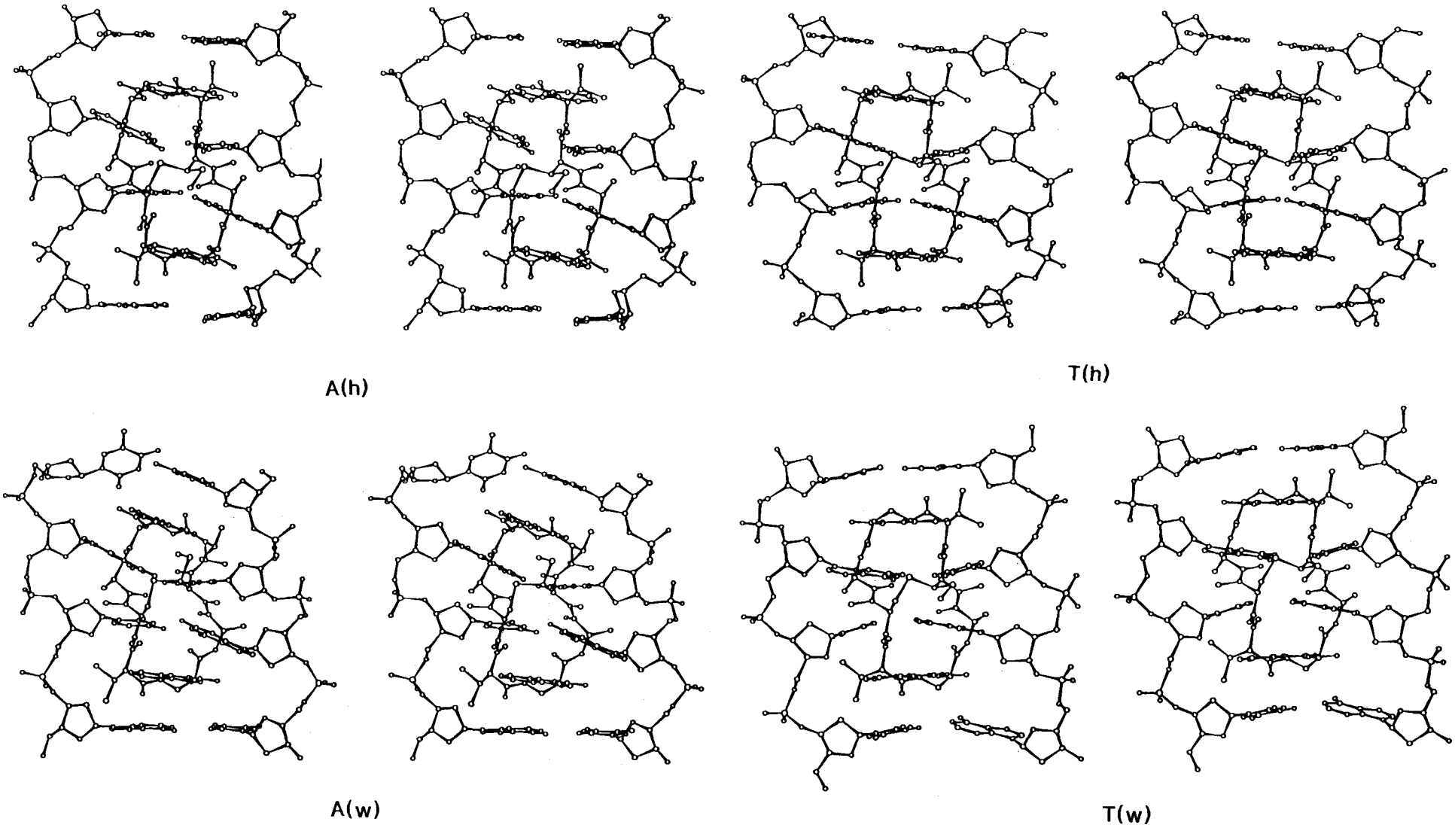

Figure 6. Stereoviews from the minor groove of the modeled A(h), A(w), T(h), and T(w) complexes upon time-averaging the atom coordinates during the last 10 ps of the unrestrained simulations in aqueous solution and further energy minimization to optimize covalent and van der Waals distances.

Table I. Solvation Free Energies (ΔG_s, kcal/mol^{-1}) for the DNA:Echinomycin Complexes, the d(ACGT)$_2$ and d(TCGA)$_2$ DNA Tetramers, and Echinomycin, Together with the Solvent Contribution to the Binding Free Energy for Each of the Complexes, $\Delta\Delta G_s$

system	ΔG_s	$\Delta\Delta G_s$
d(ACGT)$_2$	−655.1	
d(TCGA)$_2$	−667.1	
echinomycin	−24.1	
A(h)	−645.4	33.8
A(w)	−655.5	23.7
T(h)	−643.1	48.1
T(w)	−666.8	24.4

for the A(h) and A(w) complexes are partly due to these fraying effects.

NOE Distances in the Experimental A(h) and T(w) Complexes. During the unrestrained simulations in water, systematic violations of NOE's involving DNA cytosine protons and echinomycin *S*-CH_3 protons[11] were detected in both complexes. Since there is evidence that these NOE's could have arisen from either overlapping or spin diffusion effects,[22] they have not been considered in the violation lists (supplementary material). In the A(h) complex, 16 of a total of 63 NOE distances are violated. All the intramolecular echinomycin proton connectivities are maintained. Of the DNA–echinomycin NOE distances, four violations are larger than 2 Å, and all of them involve A5 and qxn-6 protons. These longer distances are due to the displacement of A5 mentioned above, which debilitates its stacking interactions with qxn-6. In the T(w) complex, only three violations are observed out of a total of 34 DNA–echinomycin NOE distances. We observe a marked asymmetry in the monitored distances at both sides of the complexes. This asymmetry has also been detected in NMR spectra[11-14] and in the crystal complex[8] but was not considered when initially applying the NOE distance constraints. Keeping in mind the qualitative nature of the NOE constraints used, these results indicate that both the A(h) and T(w) structures are reasonably near the experimentally found conformations.

(b) Solvation Free Energy of the Complexes. We have calculated the solvation free energy of the four DNA:echinomycin complexes, using structures averaged over the 30–40-ps period of the unrestrained simulations, in which van der Waals contacts and covalent distances were optimized by means of a short minimization with coordinate restraints (Table I). Calculations employing structures averaged over a shorter period of time (35–40 ps), or using fully minimized complexes, yielded the same results; test calculations using a different set of atomic radii taken from the literature[23,24] produced no significant variations in the relative stabilities (data not shown).

The solvent's electrostatic contribution to the free energy of binding, $\Delta\Delta G_s$, can be estimated from the solvation free energies of the initial and final states of the process using the relation:

$$\Delta\Delta G_s = \Delta G_{s,complex} - (\Delta G_{s,DNA} + \Delta G_{s,ech}) \qquad (2)$$

where $\Delta G_{s,complex}$, $\Delta G_{s,DNA}$, and $\Delta G_{s,ech}$ are the solvation free energies of the DNA:echinomycin complexes and those of the isolated DNA tetramers and echinomycin, respectively. The solvation term of the binding free energy favors both Watson–Crick models, A(w) and T(w), and the Hoogsteen conformation of the d(TCGA)$_2$ complex is particularly disfavored (Table I). These differences are probably induced by changes in the position of the phosphate groups attached to the terminal bases, although the composition of these bases is also an important factor, as can be seen by comparing the solvation energies of the complexed and uncomplexed d(ACGT)$_2$ and d(TCGA)$_2$ tetramers. The different behavior of the counterions around the Watson–Crick and Hoogsteen complexes strengthens the solvation results: they appear to be more stabilized around the Watson–Crick complexes, for which lower diffusion constants are found (Figure 5). This last result, however, is not conclusive because our simulations cover only 40 ps and ion equilibration probably takes times of the order of nanoseconds.

(c) Tetranucleotide Conformations and Energies. Hydrogen-Bonding Schemes and Helicoidal Parameters. The four complexes retain their initial Hoogsteen or Watson–Crick base-pairing scheme during the unrestrained simulations in water. The corresponding DNA hydrogen bonds are maintained in all the complexes, with the exceptions of base pairs A1·T8 in the A(w) complex and T4·A5 in the A(h) complex, which are partially unpaired due to the aforementioned displacements of bases T8 and A5, respectively.

Along with the changes in base pairing, the most prominent alterations brought about by echinomycin binding to DNA molecules is helix unwinding. Solution studies of DNA:echinomycin complexes have revealed an unwinding angle per echinomycin molecule of 1.9 times that of ethidium, i.e. about 50°.[25] Estimations from X-ray crystal structures have provided values ranging from 46° to 56° for echinomycin:DNA and triostin A:DNA complexes.[8-10] Unfortunately, an accurate definition of the helical axis in any of these complexed nucleotides is hampered by the important conformational changes induced by the echinomycin molecule so that only approximate values for the DNA local helical parameters can be given. For the 30–40-ps period of the unrestrained simulations in water, and by summing up the twist angles at each step, we estimate average total unwinding angles of 54°, 53°, 61°, and 70° for the A(h), A(w), T(h), and T(w) complexes, respectively.

Sugar–Phosphate Backbone Conformations. All of the NMR analyses of DNA:echinomycin complexes have found evidence that the cytosine sugars switch to C3′-endo or N-type puckering on complex formation, while the rest of the DNA residues retain a C2′-endo or S-type conformation typical of B-DNA.[11-14] On the contrary, in the crystal structures of DNA:echinomycin and DNA:triostin A, this pattern is not found, and a variety of sugar puckers is observed.[9] The pseudorotation phase angles measured in our models of the experimentally found complexes, i.e. A(h) and T(w), during the last 10 ps of the unrestrained simulations vary in a wide range with respect to the standard C2′-endo of B-DNA and experience significant fluctuations. The puckering pattern detected by NMR spectroscopy is only partially seen, and all the complexes show a general tendency for their deoxyriboses to fall in the N region of the pseudorotation cycle (supplementary material). Attempts to restrain the pseudorotation phase angles near their solution values during the simulations in water by means of a weak harmonic potential resulted in destabilization of the DNA:echinomycin complexes.

DNA Potential Energies. The Watson–Crick models of the d(ACGT)$_2$:echinomycin and d(TCGA)$_2$:echinomycin

Table II. (a) Time-Averaged Potential Energy of Each DNA:Echinomycin Complex ($V_{complex}$), and Decomposition into the Intramolecular Energies of the DNA Tetranucleotide (V_{DNA}) and Echinomycin (V_{ech}), and the DNA:Echinomycin Interaction Energy ($V_{DNA-ech}$); (b) Time-Averaged Contributions of the Individual Echinomycin Residues to $V_{DNA-ech}$[a]

(a) complex	$V_{complex}$	V_{DNA}	V_{ech}	$V_{DNA-ech}$
A(h)	-383.6 (16.5)	-227.7 (15.5)	-31.8 (5.0)	-124.1 (4.9)
A(w)	-356.2 (15.7)	-232.9 (15.7)	-27.0 (5.2)	-96.3 (8.7)
T(h)	-371.2 (28.4)	-226.7 (23.5)	-31.0 (4.9)	-113.5 (7.7)
T(w)	-378.2 (16.1)	-235.7 (14.0)	-39.9 (5.5)	-102.6 (4.5)

(b) complex	$V_{DNA-ech}$	qxn	Ala	Ser	Val	Cys
A(h)	-124.1	-60.3	-23.1	-21.9	-12.2	-6.6
A(w)	-96.3	-59.3	-13.9	-11.4	-10.0	-1.7
T(h)	-113.5	-56.7	-19.8	-17.0	-13.3	-6.7
T(w)	-102.6	-54.1	-18.8	-15.3	-8.0	-6.4

[a] All averages were calculated over the last 10 ps of the unrestrained simulations in aqueous solution. Energies are given in kcal/mol^{-1}, and the values in parentheses are standard deviations.

complexes are stabilized with respect to the Hoogsteen ones by the DNA intramolecular energy term (Table II). Singh et al. arrived at a similar conclusion in their molecular mechanics study of the d(CGTACG)$_2$:(triostin A)$_2$ complex.[19] The major contribution to the differences among the four complexes originates from local interactions between the terminal deoxyriboses and adjacent phosphate and base groups. However, the differences among the averaged DNA intramolecular energies are small compared with the large standard deviations and cannot be considered significative. This suggests that both conformations are energetically feasible for the two sequences. The fluctuations arise mainly from the interaction energy between the terminal and the central deoxyriboses, and we believe they are due to variations in sugar puckering and to an overestimation of the electrostatic energy term, partly as a consequence of the dielectric constant used (ϵ = 1). Under these conditions, subtle conformational changes are likely to cause large variations in potential energy.

(d) Echinomycin Conformations and Energies. Echinomycin Conformations. The time-averaged torsional angles of echinomycin in our models of the experimentally found complexes, A(h) and T(w), are close to those found in the X-ray structures of triostin A and echinomycin complexed with d(CGTACG)$_2$[8,9] and are consistent with the NMR results for the conformation of echinomycin in solution.[15,16] The root-mean-square fluctuations of both the atomic positions and the dihedral angles of echinomycin are lower than those found for the DNA tetramers, which is suggestive of less flexibility on the part of the antibiotic with respect to the DNA tetramers in the complexes studied (supplementary material).

The conformation of the echinomycin molecules in the two Hoogsteen complexes is similar, with a root-mean-square difference between them of 0.31 Å and is close to the X-ray conformation of echinomycin complexed to d(CGTACG)$_2$. On the other hand, the conformation of echinomycin in the Watson–Crick complexes undergoes some changes. Most notably, an intramolecular hydrogen bond is formed between the NH of one alanine (Ala-8) and the carbonyl group of the adjacent quinoxaline (qxn-6) in these two complexes (Table III). It is noteworthy that the existence of this hydrogen bond has already been proposed in one of the conformers of triostin A studied by NMR techniques in solution, based on deshielding of the Ala-NH protons.[26] A closely related hydrogen bond

Table III. 30–40-ps Average Distances (Å) and Angles (deg) for DNA:Echinomycin and Echinomycin Intramolecular Hydrogen Bonds (Labeled *)[a]

complex	donor	acceptor	distance	angle
A(h)	N (Ala-3)	N3 (G7)	2.1 (0.2)	154.6 (6.9)
	N (Ala-8)	N3 (G3)	1.9 (0.1)	159.6 (8.4)
	N2 (G7)	O (Ala-3)	2.3 (0.2)	162.6 (9.3)
	N2 (G3)	O (Ala-8)	2.2 (0.2)	160.5 (8.5)
A(w)	N (Ala-3)	N3 (G7)	2.3 (0.4)	154.6 (8.1)
	N (Ala-8)	O (qxn-6)	2.3 (0.3)	139.3 (6.8)*
	N2 (G7)	O (Ala-3)	2.4 (0.3)	146.8 (11.6)
	N2 (G3)	O (Ala-8)	2.3 (0.4)	147.5 (17.4)
T(h)	N (Ala-3)	N3 (G7)	2.0 (0.1)	157.3 (7.8)
	N (Ala-8)	N3 (G3)	2.3 (0.4)	147.5 (17.4)
	N2 (G7)	O (Ala-3)	2.4 (0.3)	161.4 (10.3)
T(w)	N (Ala-3)	N3 (G7)	2.5 (0.4)	144.7 (11.4)
	N (Ala-8)	O (qxn-6)	2.0 (0.1)	142.6 (6.9)*
	N2 (G7)	O (Ala-3)	2.3 (0.3)	157.8 (10.3)
	N2 (G3)	O (Ala-8)	2.5 (0.4)	156.2 (11.7)
	N (Ser-7)	O (Val-5)	2.1 (0.2)	135.9 (8.9)*

[a] Only hydrogen bonds with an average acceptor–hydrogen distance less than 2.5 Å and an average donor–H–acceptor angle greater than 130° are included. Values in parentheses are standard deviations.

(between the NH group of one of the alanines and a nearby quinoxaline ring N atom) has been observed in the crystal structure of triostin A[27] and has also been proposed for DNA-bound echinomycin in an NMR study.[28]

Apart from this hydrogen bond, the ester linkages of echinomycin, i.e. the CO(Val)-Oγ(Ser) atoms, are still another source of conformational variability. In the Watson–Crick complexes, the carbonyl group of one of the valines (Val-5 in T(w) and Val-10 in A(w)) points to the DNA molecule, whereas in the Hoogsteen complexes, both carbonyl groups point outwards. This asymmetry is already present in the X-ray crystal structure of triostin A complexed with d(CGTACG)$_2$.[9] As a consequence of these changes, an additional weak hydrogen bond is formed between the carbonyl group of Val-5 and the NH group of Ser-7 in the T(w) complex (Table III). In the A(w) complex, there are also changes in the orientation of the *N*-Me group of Val-10 and the CO group of Cys-9, this latter group pointing toward the DNA molecule.

Echinomycin Potential Energies. The most stable conformation of echinomycin is that adopted in the T(w) complex (Table II). The conformations of the echinomycin molecules in the Watson–Crick complexes are always favored by more negative electrostatic interactions between one of the 2-carboxyquinoxaline residues (qxn-6) and the adjacent alanine (Ala-8), mainly due to the intramolecular hydrogen bond described above. Conformational changes associated with this hydrogen bond also give rise to a better electrostatic interaction between the same 2-carboxyquinoxaline residue and the adjacent serine (Ser-7). The inverted orientation of the carbonyl group of Val-5 in the T(w) complex results in more favorable interactions with the adjacent serine residue, due to the weak hydrogen bond detected between both residues. In the A(w) complex, on the other hand, there are unfavorable interactions involving Cys-9 and Val-10, brought about by the mentioned conformational changes undergone by these residues.

(e) Echinomycin–DNA Interactions. The average interaction energies between echinomycin and the DNA tetramers during the 30–40-ps period of the unrestrained simulations in aqueous solution ($V_{DNA-ech}$) are given in Table II. In order to calculate the respective binding

enthalpies, the conformational energy change upon binding of the two molecules should be taken into account.[29] In this case, however, the relatively large standard deviations in the total energy of the complexes ($V_{complex}$) arise mainly from fluctuations in the intramolecular energy of the DNA tetramers (V_{DNA}). Besides, we do not wish to speculate on the conformation of the DNA tetramers prior to binding of the drug. Having this in mind, the DNA–echinomycin interaction energies ($V_{DNA-ech}$) are compared. As implied by the experimental results,[13,17,28] the Hoogsteen conformation of the d(ACGT)$_2$ complex is found to be significantly favored over the rest. On the contrary, the experimentally found Watson–Crick conformation for the TCGA sequence appears to be enthalpically destabilized relative to its Hoogsteen counterpart.

In order to delineate the contribution of the different echinomycin residues to the total interaction energy, the time-averaged interaction energies of each residue with the DNA molecule are also shown in Table II. A detailed analysis of these energies has been performed, delimiting the average contributions of the different nonbonded terms for each residue and also the average contributions from each half of the complexes (data not shown). We note that the drug does not interact symmetrically with the two strands of the DNA tetramers. This fact is in consonance with previous experimental[11-14] and theoretical[19] studies.

The three major types of interaction that echinomycin establishes with the DNA molecules will be discussed separately: (1) van der Waals and electrostatic interactions between the depsipeptide part of the drug and the minor groove of the DNA molecules, (2) hydrogen bonds between the alanine residues of echinomycin and the guanine bases of DNA, and (3) stacking interactions between the quinoxaline chromophores and the adjacent base pairs.

(1) Depsipeptide–DNA Interactions. The Hoogsteen conformation in both sequences is stabilized by more favorable interactions of the "terminal" residues of the depsipeptide, i.e. valines and serines, with the DNA molecules (Table II). Singh et al.[19] concluded that the van der Waals interaction between the valine residues and the DNA molecule was the main factor stabilizing the Hoogsteen conformation of the d(CGTACG)$_2$:(triostin A)$_2$ complex. This was considered to be a consequence of the narrowing of the DNA minor groove (about 2 Å) in the complex adopting the Hoogsteen conformation. We likewise detect a van der Waals stabilization of about 3 kcal mol^{-1} in the Hoogsteen complexes, but located at the serine residues instead. This finding is in agreement with the NMR spectra of the A(h) and T(w) complexes:[11] whereas the valine–DNA contacts are maintained in both complexes, serine–DNA NOE's are only detected in the Hoogsteen complex. Another factor contributing to this interaction energy difference is found to be an unfavorable electrostatic interaction of the valine carbonyl group facing the DNA in the Watson–Crick models.

The differences in the alanine–DNA interaction energies are mainly due to the electrostatic and hydrogen bonding terms, as the van der Waals term is very similar in the four complexes studied. The cysteine residues interact the least with the DNA tetramers, and their role appears to be mainly structural, providing rigidity to the cyclic depsipeptide. The particularly low interaction energy value for this residue in the A(w) complex is due to the unfavorable electrostatic interaction of Cys-9, whose carbonyl group is pointing toward the DNA tetramer.

(2) Echinomycin–DNA Hydrogen Bonds. In agreement with NMR and X-ray results, echinomycin hydrogen bonds to the guanine bases of the DNA tetramers through the NH and CO groups of its alanine residues (Table III). In the A(h) model, there are two strong hydrogen bonds between the amino groups of alanines and N3 of guanines and two more between the carbonyl groups of alanines and the 2-amino groups of guanines, one of which is only slightly weaker due to the asymmetrical binding of echinomycin. In contrast, in the T(h) complex the hydrogen bond between the carbonyl group of Ala-8 and the 2-amino group of G3 is lost. In the Watson–Crick complexes, on the other hand, the NH group of Ala-8 hydrogen bonds to the carbonyl group of the adjacent quinoxaline residue (qxn-6), as described previously. The amino group of Ala-3 maintains the hydrogen bond to N3 of G7, and the same occurs between the carbonyl groups of both alanines and the amino groups of the nearby guanine residues.

The loss of one intermolecular hydrogen bond in T(h) and both Watson–Crick models is reflected in the lower interaction energies of their alanine residues with DNA and contributes to explaining the higher binding affinity of echinomycin for the ACGT sequence in a Hoogsteen conformation.

(3) Stacking Interactions. The quinoxaline residues contribute notably (nearly 50%) to the total interaction energy between echinomycin and the DNA tetramers (Table II). Since it is generally accepted that the *flanking* sequence specificity of the antibiotic rests largely on the aromatic stacking interactions of the quinoxaline chromophores,[11-14,17,28] a detailed analysis of these interactions in the four models studied was performed.

The dependence of DNA stacking interactions on the composition and *orientation* of the nucleic acid bases has been shown to be largely dominated by the electrostatic term, the van der Waals contribution being rather indiscriminate in comparison.[30] The reason for this lies on the polarity of the charge distributions, which is conveniently represented by the dipole moment. On the other hand, and according to NMR and X-ray results, the quinoxaline chromophores stack preferentially between the adenine and cytosine bases in the ACGT sequence, whereas the stacking is between the thymine and cytosine bases in the d(TCGA)$_2$ complex (Figure 8). However, the 2-carboxamide groups attached to the quinoxaline rings of echinomycin, which have received little attention, must also be taken into account when considering echinomycin–DNA stacking interactions, as they are coplanar and conjugated with the quinoxaline rings. Therefore, we consider that not only the quinoxaline rings, but the entire quinoxaline-2-carboxamide conjugated systems do participate in the stacking interactions, which thus overlie the *whole adjacent base pairs*, as can be seen in Figure 8.

Following this reasoning, the dipole moments ($\vec{\mu}$) of the AT and GC base pairs and that of the quinoxaline-2-carboxamide chromophore of echinomycin were calculated according to eq 3 using the charges (q) and positions ($\vec{r}$) of the atoms of each of the systems.

$$\vec{\mu} = \sum_{i=1}^{n} q_i \vec{r}_i \qquad (3)$$

Note that for the dipole moment to be independent of the

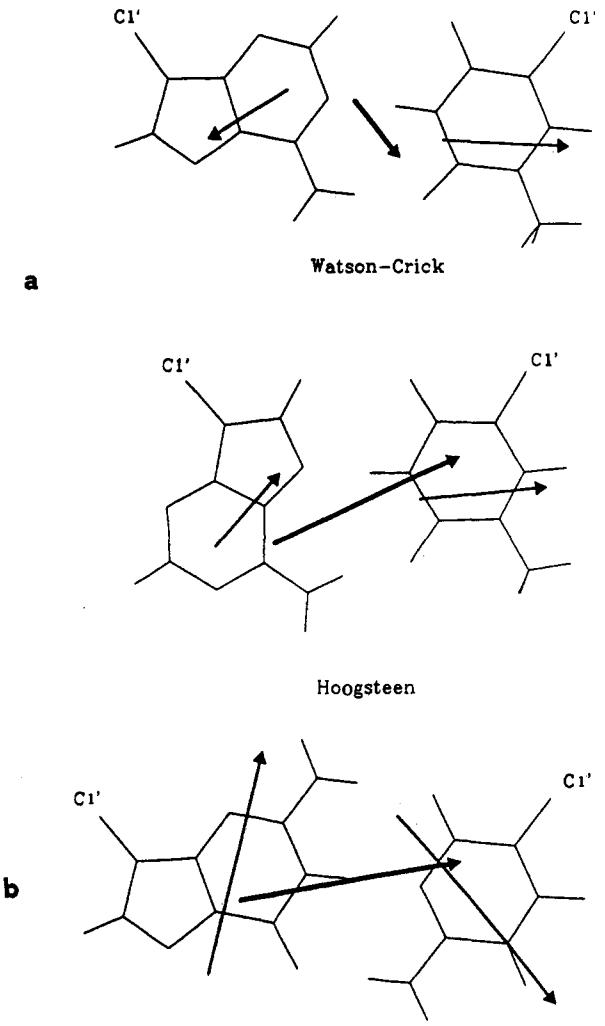

Figure 7. Dipole moments (thick arrows) of (a) a standard AT base pair in either a Hoogsteen or a Watson–Crick conformation and (b) a standard GC base pair in a Watson–Crick conformation. The dipole moments of individual bases are drawn as thin arrows. The midpoint of each vector is centered on the geometrical center of the system considered.

origin of coordinates, the sum of charges must be zero. Therefore, C1′ atoms of DNA and C_α atoms of serines were included in the calculations to be used as buffers in order for each of the systems to achieve electrical neutrality. Consequently, the charges of these atoms where modified to values of 0.0550 and 0.1625 for C1′ of DNA and C_α of serines, respectively. The rest of the charges correspond to those used in the molecular mechanics force field (ref 31 and supplementary material). The dipole moments for the same molecular fragments (after filling the valences of C1′ and C_α with hydrogens) were also calculated by using the semiempirical AM1 and PM3 hamiltonians within the MOPAC program[32] and compared with available experimental data (Table IV).

In our modeled complexes, the dipole moments of the same systems were likewise calculated according to eq 3 and monitored during the 30–40-ps interval of the unrestrained simulations in water. The corresponding dipole–dipole interaction energies, V_{dip} (Table V), were also calculated over the same period of time by means of eq 4

$$V_{dip} = \epsilon^{-1}\left[\frac{\vec{\mu}_1\cdot\vec{\mu}_2}{\vec{r}^3} - \frac{3(\vec{\mu}_1\cdot\vec{r})\,(\vec{\mu}_2\cdot\vec{r})}{\vec{r}^5}\right] \quad (4)$$

where $\vec{\mu}_1$ and $\vec{\mu}_2$ are the dipole moment vectors, $\vec{r}$ is the vector that separates them, and ϵ is the relative permittivity of the medium, taken to be 1. From the results shown in Tables IV and V, three interesting remarks can be made:

(1) On Hoogsteen base pair formation, the dipole moment of an AT base pair increases from a value of about 2 D found for the Watson–Crick conformation to more than 5 D (Table IV). This is a consequence of the rotation of the adenine ring around the glycosidic bond to adopt the syn conformation: in this orientation, the adenine dipole adds to the thymine one, whereas in the Watson–Crick arrangement both dipoles tend to cancel each other (Figure 7).

(2) The quinoxaline-2-carboxamide chromophores of echinomycin have a high dipole moment of 4–5 D (Table IV): the negative pole is located on the pyrazine-2-carboxamide region whereas the positive one is on the benzene ring region (Figure 8).

(3) In the experimentally found A(h) complex, the high dipole moment of each AT base pair in a Hoogsteen conformation and that of the stacked echinomycin chromophore have opposite directions, which gives rise to a favorable dipolar interaction. On the contrary, the dipole moment of the AT base pair reverses its orientation in the nonexperimental Hoogsteen complex T(h), so that both dipole vectors point in the same direction, and therefore the dipolar interaction is unfavorable (Figure 8). In the Watson–Crick models, on the other hand, the dipolar interactions are weaker due to the lower dipole moment of the AT base pairs in this arrangement. Therefore, as regards the electrostatic stacking interactions with the terminal AT base pairs, this means that a Hoogsteen base pair scheme should be preferred for binding of echinomycin to the $d(ACGT)_2$ tetramer, whereas the classical Watson–Crick hydrogen bonding pattern would be more stable for the TCGA sequence. This is precisely what is detected experimentally.

The van der Waals contribution to the stacking energy (V_{vdw}) was calculated by using the same groups of atoms as for the evaluation of the electrostatic component and is also shown in Table V. As regards the terminal AT base pairs, this interaction is almost similar in the A(h) and A(w) models, but it favors the experimentally found T(w) over T(h). These observations can be tested by visual inspection of Figure 8, where the adenine of the T(h) complex has virtually no stacking with the echinomycin chromophore.

Because eq 4 assumes point dipoles, the distance between interacting dipoles should be long relative to the length of the dipole vectors. In the echinomycin–DNA models, dipoles of the order of 1 e·Å are separated by distances of about 3.5 Å; hence the values given by this equation are only approximate. The point-charge approximation has also been used for calculating the electrostatic interactions between the DNA base pairs and the echinomycin chromophores (V_{pch}), utilizing the same set of charges used to calculate the dipole moments. The absolute values obtained using one method or the other differ but the differences reported above remain (Table Va): in the A(h) model, the point-charge electrostatic stacking energy between the echinomycin chromophores and the AT base pairs is more favorable than in the rest of the complexes. The total stacking energies (V_{stack}) were obtained by summing up the van der Waals term and the point charge

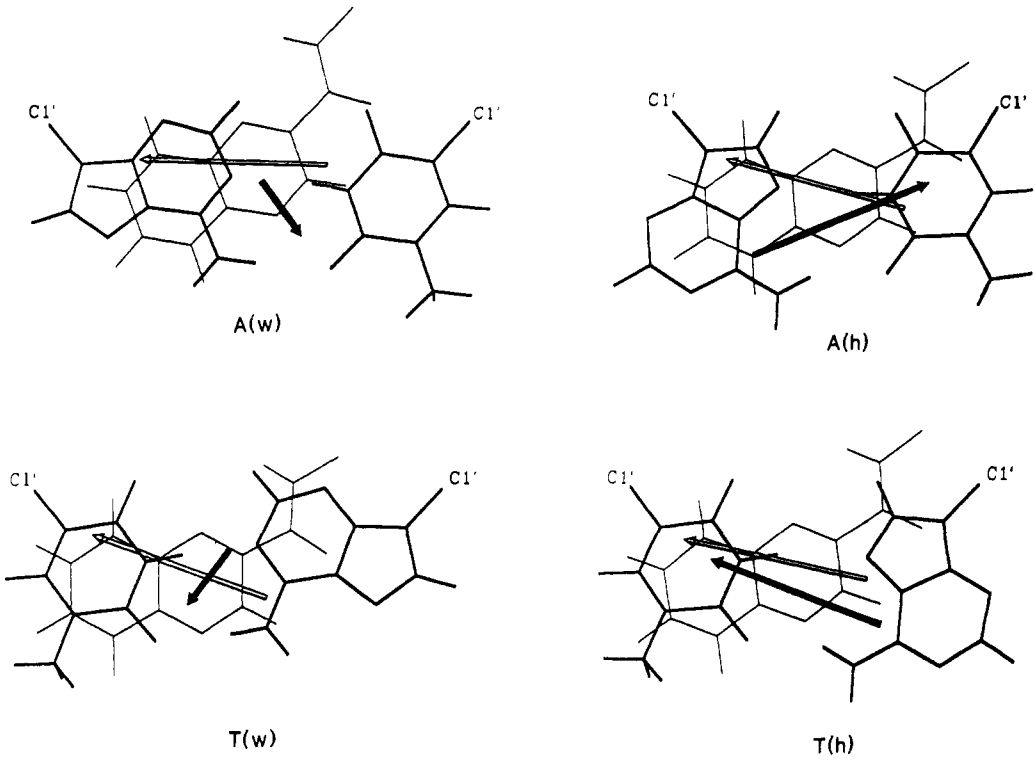

Figure 8. Stacking interactions between the quinoxaline-2-carboxamide chromophores of echinomycin and the terminal AT base pairs of the complexes. The structures were taken from the optimized 30–40-ps averaged coordinates. Top: A(w) (left) and A(h) (right). Bottom: T(w) (left) and T(h) (right). The dipole moments of the AT base pairs and the echinomycin chromophores are represented by filled and unfilled arrows, respectively. It can be seen that for both sequences the most favorable dipole coupling is displayed by the models of the experimentally found conformations, i.e. A(h) and T(w).

Table IV. Dipole Moments (in Debyes) of the Quinoxaline-2-carboxamide System of Echinomycin (qxn–CONH), the Individual DNA Bases, and Standard GC and AT Base Pairs in either Watson–Crick (w) or Hoogsteen (h) Conformation[a]

system	μ_{MEP}	μ_{PM3}	μ_{AM1}	μ_{exp}
qxn–CONH	5.23	3.85	3.78	
N9–Me–A	2.22	2.23	2.27	3.25 ± 0.20
N1–Me–T	3.14	4.24	4.50	4.07 ± 0.02
N9–Me–G	5.37	6.28	6.52	
N1–Me–C	5.71	5.86	6.03	4.29 ± 1.4[b]
GC (w)	5.08	6.81	5.98	
AT (w)	1.74	1.51	2.34	2.31[c]
AT (h)	5.08	5.87	6.37	6.82[c]

[a] They were calculated using eq 3 and the molecular electrostatic potential-derived charges employed in the force field, as explained in the text (μ_{MEP}), or by using MOPAC with either the AM1 (μ_{AM1}) or PM3 (μ_{PM3}) Hamiltonians. The quantum mechanics calculations were performed on the N1 or N9 methylated bases (N9–Me–A, N1–Me–T, N9–Me–G, and N1–Me–C) and the *N*-methylquinoxaline-2-carboxamide system. For comparison, the available experimental dipole moments of the methylated bases, taken from ref 33, are also given (μ_{exp}). Additionally, the dipole moment of the AT base pair in either a Watson–Crick or a Hoogsteen conformation was calculated from the experimental values of the individual bases, taking as the vector direction for each base that found for the respective μ_{MEP}. [b] Value found for 1–H–cytosine, not N1–Me–C. [c] Estimated from the experimental values of N9–Me–A and N1–Me–T.

electrostatic term (V_{pch}) and again favor the models of the experimentally found complexes, A(h) and T(w), over A(w) and T(h).

The stacking interactions between the echinomycin's chromophores and the GC base pairs were also calculated by using the same methods (Table Vb). As expected, these interactions are similar in the four models. The dipole moment of a GC base pair in a Watson–Crick conformation is notably high (about 5 D, Table IV and Figure 7) and points in the same direction as that of the quinoxaline-2-carboxamide group. This yields an unfavorable electrostatic stacking interaction between both groups, as can be seen from the results shown in Table Vb for V_{pch} and V_{dip}. This is not surprising if one recalls that in the crystal complexes of DNA with either echinomycin or triostin A, distances in the 3.7–4.0-Å range found between the chromophores and the GC base pairs, as opposed to 3.5 Å with respect to the AT base pairs,[8,9] imply that the stacking interactions between echinomycin and the GC base pairs are rather weak. Furthermore, if echinomycin were to bind to GpC rather than to CpG, the stacking interactions would improve, but at least the hydrogen bonds involving the carbonyl groups of alanines would be lost. The same reasoning applies to a hypothetical TpA binding site. Here the electrostatic term of the stacking interaction with the sandwiched AT pairs would also be improved because of the lower dipole moment of an AT pair in a Watson–Crick conformation relative to a GC pair, but again the amino groups in the DNA minor groove ready to hydrogen bond to the carbonyls of alanine would not be present. This factor may account for the binding selectivity of TANDEM for TpA sites.[2,34,35] In TANDEM, a triostin A analogue lacking the *N*-methyl groups of cysteines and valines, the carbonyl groups of the alanines

Table V. Stacking Energies (kcal/mol^{-1}) between the Echinomycin Chromophores and the AT (a) and GC (b) Base Pairs of the DNA Tetramers, Averaged over the 30–40-ps Interval of the Unrestrained Simulations in Water[a]

complex	V_{stack}	V_{vdw}	V_{pch}	V_{dip}	θ
	(a) AT Base Pairs: qxn–CONH				
A(h)	−27.5	−23.5	−4.0	−7.6	141.1
A(w)	−26.1	−23.9	−2.2	−2.2	117.0
T(h)	−26.1	−25.2	−0.9	8.5	17.9
T(w)	−27.6	−26.0	−1.6	4.0	51.7
	(b) GC Base Pairs: qxn–CONH				
A(h)	−26.8	−27.7	0.9	19.2	15.4
A(w)	−25.2	−27.3	2.1	14.5	25.5
T(h)	−25.9	−27.2	1.3	16.6	16.8
T(w)	−24.5	−26.3	1.8	17.7	28.7

[a] The electrostatic term of the stacking energy was obtained by means of either a point-charge interaction model (V_{pch}) or a dipole–dipole interaction model (V_{dip}). The dipolar interactions were monitored using eqs 3 and 4, as explained in the text. V_{vdw} is the van der Waals contribution to the stacking energy. V_{stack} is the total stacking energy ($V_{vdw} + V_{pch}$). All the energy values result from summing up the corresponding stacking interactions at both sides of the complexes. θ is the angle (in degrees) formed between the dipole moment vectors of the base pairs and the quinoxaline-2-carboxamide systems, averaged over both sides of the complexes. All the magnitudes are time averages over the last 10 ps of the unrestrained simulations in water.

hydrogen bond to the NH groups of the valines and hence are thought not to interact with DNA.[5,35] The preference of this drug for TpA sites over CpG sites, both of them having the N3 group of purine in the minor groove ready to hydrogen bond to the free NH groups of alanines, may arise from the more favorable stacking interactions of the drug in the TpA binding site, irrespective of the flanking sequences. Thus, the DNA binding specificity of the quinoxaline antibiotics appears to be the result of a subtle balance between stabilizing and destabilizing forces. The strong affinity of echinomycin for CpG steps is decisively determined by a number of hydrogen bonds between its alanine residues and both the N3 and 2-amino groups of guanine, because the electrostatic component of the stacking interactions between its chromophores and the CpG step is unfavorable. When the hydrogen-bonding capabilities of the antibiotic are partially lost but the chromophores remain unchanged, as occurs in TANDEM, the binding specificity of the drug changes. The more favorable dipolar stacking interactions would make GpC and ApT, in this order, the best targets for TANDEM binding (cf. dipole moments and directions in Figure 7). Experimentally, however, it is the TpA step that is preferentially sandwiched between the quinoxaline chromophores of this drug.[2] This effectively means that N3 of adenine is preferred over O2 of either cytosine or thymine for hydrogen bonding and that the magnitude of this interaction overrides the selectivity imposed by the dipolar stacking interactions toward GpC and ApT (but not toward CpG).

As is the case with AT pairs, when GC pairs flank the echinomycin CpG binding step, Hoogsteen base pairing is only observed (at acidic pH) if the purine base (guanine) is on the 5′ side of the CpG sites, i.e. it is detected in d(GCGC)$_2$ and d(GCGTACGC)$_2$, but not in d(CCGG)$_2$.[10,12] The Hoogsteen hydrogen bonding scheme in GC pairs requires the protonation of the cytosine base.[10,12] For this reason, we believe that the Hoogsteen arrangement appears in the two alternating sequences because the positively charged cytosines are located on top of (or below) the negative pole of the quinoxaline-2-carboxamide systems, giving rise to a favorable electrostatic interaction. In a hypothetical Hoogsteen d(CCGG)$_2$:echinomycin complex, the opposite situation would emerge and the stacking interaction would be electrostatically destabilized. Further work is in progress to test this hypothesis.

Different studies have shown the influence of chromophore composition on the DNA-binding specificity of echinomycin-like antibiotics.[17,36,37] Minor modifications on the quinoxaline ring such as replacement of a ring nitrogen with a carbon[17,36] (quinoline analogues) or substitution at the 3 position[37] (3-amino-quinoxaline analogues) cause striking variations in flanking sequence specificity. This is consistent with the described predominant role of the electrostatic term in the stacking interactions. We have evaluated the importance of this term by calculating the reorientational time correlation functions between the dipole vectors of the DNA base pairs ($\vec{\mu}_{AT}$, $\vec{\mu}_{GC}$) and the dipole vectors of the quinoxaline-2-carboxamide systems ($\vec{\mu}_{qxn-CONH}$). The movements of $\vec{\mu}_{AT}$ and $\vec{\mu}_{qxn-CONH}$ appear to be more coupled in the Hoogsteen complexes, in which the dipolar interactions between these two systems are more intense, than in A(w) or T(w); the movements of $\vec{\mu}_{GC}$ and $\vec{\mu}_{qxn-CONH}$ are highly correlated in the four complexes (data not shown).

In all of the oligonucleotide:echinomycin complexes studied so far, the *terminal* base pairs adjacent to the echinomycin CpG binding steps are stably Hoogsteen base paired when the purine base is on the 5′ side of the CpG sites. However, this picture is much less clear at *internal* positions, where structural constraints can prevent the purines from rotating into the syn conformation. This can be the case in the d(AAACGTTT)$_2$:echinomycin complex[12] and in a complex of a 3-hydroxyquinaldic analogue of echinomycin with d(GACGTC)$_2$[38] where no Hoogsteen pairs are detected in the NMR experiments. A different situation appears when two CpG binding steps are separated by an *alternating* tract of AT pairs, as in the complexes of echinomycin with d(ACGTACGT)$_2$, d(ACGTATACGT)$_2$, and d(TCGATCGA)$_2$ studied by NMR spectroscopy.[13,14] In all of these three complexes, the unwinding induced by the drug is propagated to the central AT pairs. In contrast, echinomycin only binds cooperatively to the sequences where the adenines are on the 5′ side of the CpG steps, i.e. d(ACGTACGT)$_2$ and d(ACGTATACGT)$_2$. Furthermore, the central AT pairs are only observed to be destabilized relative to free DNA in the complexes of echinomycin with these two sequences. In the first one, Hoogsteen base pairs are transiently formed in the two central AT pairs at physiological temperature. In the second one, no Hoogsteen pairs are detected but the destabilization persists. On the contrary, in the d(TCGATCGA)$_2$:echinomycin complex no Hoogsteen base pairs are observed at any temperature, the central AT pairs are stabilized with respect to unbound DNA, and no binding cooperativity is detected. We believe that transient Hoogsteen base pairing in the *unwound* central AT pairs contributes to explaining the observed binding cooperativity of echinomycin to d(ACGTACGT)$_2$ and d(ACGTATACG)$_2$ and can account for the destabilization of the central AT pairs. When the internal AT pairs adopt a Hoogsteen scheme, an exothermic arrangement of dipole vectors appears, as represented in Figure 9A. Binding cooperativity could then arise from an enhanced electrostatic (and probably van der Waals) stacking interaction *between these central unwound AT base pairs in a*

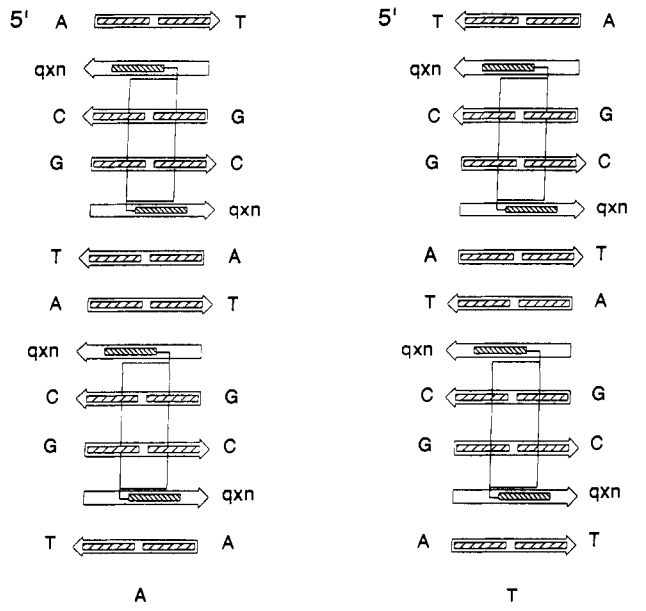

Figure 9. Dipolar coupling in the complexes of echinomycin with the $d(ACGTACGT)_2$ (A) and $d(TCGATCGA)_2$ (T) octamers, *assuming a Hoogsteen conformation* for the AT pairs adjacent to the echinomycin CpG binding steps. Note the favorable dipolar interactions in complex A, which may account, at least in part, for the higher affinity and cooperativity of echinomycin binding to this sequence. In contrast, no Hoogsteen pairs are likely to occur in complex T as a consequence of unfavorable dipolar interactions between the AT base pairs and the quinoxaline-2-carboxamide system.

Hoogsteen conformation. In relation to this, a significant enhancement of the stacking interaction between the central Hoogsteen-paired AT base pairs with respect to the Watson–Crick arrangement was reported by Singh et al.[19] in their molecular mechanics study of the $d(CGTACG)_2$:(triostin A)$_2$ crystal complex. On the contrary, Hoogsteen AT base pairing in the complex of echinomycin with $d(TCGATCGT)_2$ would generate a different and unfavorable dipole–dipole interaction scheme (Figure 9T) and hence the Watson–Crick conformation would be favored for the central AT base pairs: in this complex, no cooperativity is detected and the central AT base pairs remain Watson–Crick paired and are stabilized relative to free DNA.[13] Nonalternating AT base pairs separating the echinomycin binding CpG sites, as in $d(CGAACG)_2$ or $d(CGTTCG)_2$, would also result in unfavorable stacking patterns and we predict they should be weaker and noncooperative binding sequences for echinomycin. Note that the same reasoning can be applied to $d(AAACGTTT)_2$: echinomycin, where no Hoogsteen base pairs are detected.[12] A molecular dynamics study of echinomycin complexed to $d(ACGTACGT)_2$ and $d(TCGATCGA)_2$ is currently underway to evaluate these hypotheses.

Much more difficult is the extrapolation of our results to the binding of echinomycin to longer and more complex DNA tracts, as those studied in footprinting experiments. AT-rich sequences flanking echinomycin binding sites have been shown to become hyperreactive to diethyl pyrocarbonate[39,40] and OsO_4,[41] and more susceptible to cleavage by DNase I,[6] which is indicative of some type of conformational change cooperatively propagated as a consequence of echinomycin binding. This conformational change has been proposed to be either Hoogsteen base pairing[39] or unwinding of the DNA helix.[14,41] Hoogsteen pairing does not appear to account for the described changes: adenines on the 3′ side of the echinomycin binding site, in which Hoogsteen base pairing is not likely to occur, are also found to be hyperreactive to diethyl pyrocarbonate.[39,40] Furthermore, DNA sequences with the adenines modified such that they cannot form Hoogsteen pairs have been shown to remain hypersensitive to OsO_4.[41] Unwinding per se, on the other hand, cannot explain the described changes either.[40] Thus, we tend to think that local unspecific unwinding or local transient Hoogsteen pairing (sequence specific) in base pairs adjacent to CpG echinomycin binding steps might serve as a catalyst to cause cooperative changes of unknown nature in AT-rich sequences adjacent to echinomycin binding sites.

Conclusions

Two different hydrogen bonding schemes are possible for the AT base pairs flanking the central CpG binding site in the complexes of echinomycin with the DNA tetramers $d(ACGT)_2$ and $d(TCGA)_2$, giving rise to four different models which have been analyzed by theoretical methods. The Hoogsteen scheme in $d(ACGT)_2$:echinomycin has been found to be clearly favored over the rest by the DNA–echinomycin interaction energy, as implied by the experimental results.[13,17,28] In this complex, more favorable stacking interactions between the echinomycin chromophores and the flanking AT pairs were found, together with better hydrogen bonding interactions between the alanine residues and the guanine bases, and more negative interactions of the valine and serine residues with atoms of the minor groove of the DNA tetramer.

Our calculations suggest a large increase of the dipole moment of an AT base pair in the Hoogsteen conformation relative to the dipole moment of the same base pair with a Watson–Crick hydrogen bonding scheme. Favorable dipolar interactions between the Hoogsteen AT base pairs and the quinoxaline-2-carboxamide chromophores of echinomycin contribute to explaining why Hoogsteen AT pairs are detected in the complex of echinomycin with $d(ACGT)_2$.

On the other hand, a Hoogsteen rearrangement at the terminal AT pairs in $d(TCGA)_2$:echinomycin would lead to unfavorable dipolar interactions. Since the Watson–Crick models are stabilized relative to the Hoogsteen models, both by the intramolecular DNA potential energy and by the solvent contribution to the binding free energy, the sum of these factors can account for the observed preference of $d(TCGA)_2$:echinomycin for a Watson–Crick conformation.

The electrostatic term of the stacking interactions with the sandwiched base pairs can also account for the reported affinity of TANDEM for TpA steps. For these reasons, modulation of the dipole moment of the intercalating chromophores can be an additional element to be considered when sequence-specific DNA intercalators are to be designed. Modeling studies of this kind should benefit from the inclusion of multipole interactions as well as of induction effects in the electrostatic term of the molecular mechanics force field. These matters deserve further investigation.

Methodology

The AMBER 3.0 Rev. A and AMBER 4.0 suites of programs[42] were used throughout, implemented on Cyber 910B-537, Cyber 910B-480, and Silicon-Graphics INDIGO workstations. The INSIGHT II molecular graphics software[43] was used to visualize and manipulate the structures.

(1) Model Building. The initial coordinates used in the model building process were those published for the d(GCGTACGC)$_2$ octamer complexed with two molecules of triostin A.[10] This system was chosen for three main reasons: (1) the coordinates of the d(CGTACG)$_2$:(echinomycin)$_2$ complex[8] have not been published; (2) there is a high degree of similarity between the DNA crystal complexes of echinomycin and triostin A;[8] and (3) more importantly, this crystal structure is the only one presently available having terminal base pairs on both sides of the antibiotic's chromophores, thereby providing critical information regarding the rise and twist parameters of such base pairs, and consequently about their stacking interactions with the quinoxaline chromophores.

A(h), A(w), T(h), and T(w) were built by making the appropriate modifications of base composition and base pairing scheme on one of the symmetrical halves of the mentioned crystal complex. Triostin A was replaced with echinomycin by transforming the disulfide linkage into a thioacetal bridge, taking into account the results of Williamson and Williams[16] about the absolute chirality (*S*) of the asymmetric carbon and the conformation of the methylene groups in the thioacetal cross bridge.

(2) Assignment of Force Field Parameters. The AMBER all-atom force field parameters[31] were used for the DNA tetramers and the standard aminoacid residues of echinomycin. The water molecules were modeled by the rigid three-point charge TIP3P model.[44] The van der Waals parameters for the sodium counterions corresponded to those derived by Aqvist[45] from free energy perturbation simulations. Covalent parameters for the quinoxaline chromophores of echinomycin were derived, by analogy or through interpolation,[46] from those already present in the AMBER database. The parameters for the ester linkage between D-serine and *N*-Me-valine residues and for the thioacetal cross-bridge were calculated by a combination of molecular mechanics and quantum mechanics calculations, following the method proposed by Hopfinger and Pearlstein[47] (supplementary material).

The charge distribution for each of the nonstandard residues of echinomycin (i.e. 2-carboxyquinoxalines, D-serines, *N*-methylvalines, *N*-methylcysteine, and *S*,*N*-dimethylcysteine) was derived by fitting the quantum mechanically calculated molecular electrostatic potential to a point charge model.[48] For the N-methylated amino acids, point charges were calculated for the peptide backbone atoms while standard charges were assigned to the side chain atoms, using the β carbons as buffers when necessary. This procedure was used by Weiner et al. for amino acid charge derivation[31,46] and yields point charges consistent with those present in the AMBER database (supplementary material).

(3) Generation of the Initial Conformations. In order to obtain reliable initial conformations for the dynamics simulations in solution, we made use of data derived from the NMR analysis of the complexes of echinomycin with d(ACGT)$_2$ and d(TCGA)$_2$.[11] Although the lists of reported NOE intensities had only a qualitative intent and do not account for the asymmetry of the complexes, they should be of value to obtain initial structures close to the experimentally found ones. This is particularly true for the Watson–Crick complexes, for which there is no other conformational information available. Thus, the two sets of NOE's reported by Gao and Patel[11] for the complexes of echinomycin with d(ACGT)$_2$ (Hoogsteen-paired terminal base pairs) and d(TCGA)$_2$ (Watson–Crick-paired terminal base pairs) were converted to distance constraints. The conformation of each of the other two systems was taken to be similar to that found for the alternative sequence with identical base pairing scheme, and the corresponding set of distances was assigned, except for the NOE's involving protons of the terminal DNA bases. By using the SANDER module of AMBER 4.0, the NOE distances were included in the force field as extra terms with the form of a flat well with parabolic sides:

$$V_{NOE} = K_{NOE}(r - r_u)^2 \qquad \text{if } r > r_u$$

$$V_{NOE} = 0 \qquad \text{if } r_l \le r \le r_u$$

$$V_{NOE} = K_{NOE}(r - r_l)^2 \qquad \text{if } r < r_l \qquad (5)$$

where K_{NOE} is the NOE restraint force constant and r_l and r_u are the lower and upper limits of the distance constraints, which were assumed to be 2–3, 3–4, and 4–5 Å for strong, medium, and weak NOE's, respectively. For the intramolecular distance connectivities among echinomycin protons in the Hoogsteen complexes,[11] r_l and r_u were assigned values of 2 and 5 Å, respectively. The sides of the restraining functions were turned into linear 0.5 Å away from the upper and lower limits. Hydrogen bonds between the NH groups of alanine and the N3 atoms of guanine were unambiguously detected in the NMR spectra of both complexes and were therefore also included as distance restraints with an equilibrium distance of 2.8 ± 0.2 Å. An equilibrium donor–acceptor distance of 2.9 ± 0.1 Å was likewise assigned to the hydrogen bonds between the DNA bases. The initial force constant value (K_{NOE}) was 50 kcal mol^{-1} Å^{-2} for all the constraints.

Within the framework of this modified force field, the initial models were refined by progressively minimizing their potential energy: firstly the sugar–phosphate DNA backbone and the peptide part of the antibiotic and then the whole system. Before each minimization step, a short optimization run constraining the atoms to their initial coordinates allowed readjustment of covalent and van der Waals contacts without changing the overall conformation of the complexes. The optimizations were carried on in a continuum medium of relative permitivitty $\epsilon = 4r_{ij}$,[49] and the nonbonded interactions were calculated within a 15-Å cutoff. The optimized structures were thereafter subjected to a restrained molecular dynamics simulation lasting 20 ps, under the same conditions as before and with a time step of 1 fs. The systems were coupled to a heat bath with a time relaxation constant of 0.1 ps. During the first 3 ps, the temperature was raised to 300 K in steps of 100 K over 1-ps blocks, the atomic velocities being scaled whenever the temperature deviated from the reference value by more than 10 K. The complexes were then further equilibrated at 300 K for the remaining 17 ps. In the 5–10-ps interval, K_{NOE} was increased from its initial value of 50 to a maximum value of 200 kcal mol^{-1} Å^{-1} by linear interpolation. Coordinates from the last 5 ps were saved every 0.1 ps, averaged and subjected to restrained energy minimization to generate the final structures. The minimizations were carried out following the same procedure as above, first the hydrogens atoms alone and then the whole systems. The final value of 200 kcal mol^{-1} Å^{-1} for K_{NOE} has been used in other restrained dynamics simulations of DNA[50] and ensured average distance restraint violations of less than 0.1 Å in all complexes, with a maximum standard deviation of 0.1 Å.

For these restrained simulations in vacuo, we found it necessary to constrain the AT terminal bases in all the complexes to their initial coordinates in order to avoid fraying effects. This was accomplished by applying a harmonic force constant of 3 kcal mol^{-1} Å^{-2}. The DNA dihedrals of the Hoogsteen complexes were also constrained to their crystallographic values with harmonic functions which switched to linear 30° away from the equilibrium values. For the terminal AT base pairs of the Watson–Crick complexes the sugar and phosphate backbone dihedrals found in the corresponding bases of the d(CGTACG)$_2$:(daunomycin)$_2$ crystal complex[51] were used as equilibrium values, as this is one of the nearest Watson–Crick DNA:intercalator complexes for which detailed conformational information is available. The torsion restraint force constants were assigned values similar to those used for the distance restraints. This procedure was adopted after a considerable number of exploratory calculations, in which end effects gave rise to instabilities at the terminal AT base pairs during the subsequent simulations in water.

(4) Molecular Dynamics Simulations in Aqueous Solution. Once the initial structures were obtained in a conformation as close as possible to the conformations experimentally found in solution, a molecular dynamics study of the complexes in water was undertaken *without using any constraints*, so as to let each of the systems evolve freely. In order to include the effects of solvation explicitly, the complexes were placed in the center of rectangular boxes with dimensions such that the minimum distance between any atom in the complexes and the wall of the boxes was 6 Å. Water molecules were inserted in the box by immersing it into a Monte Carlo-equilibrated configuration of TIP3P water molecules[44] and by subsequently removing all water

molecules that were outside the box or whose oxygen or hydrogen atoms lay within 2 or 1 Å, respectively, of any DNA or echinomycin atom. This procedure yielded systems with 724, 699, 666, and 732 water molecules for the A(h), A(w), T(h), and T(w) models, respectively, on which periodic boundary conditions were applied. For the nonbonded interactions, a dielectric constant of 1 and a cutoff of 8 Å were used. This latter value has proved acceptable in previous simulations of this kind[3,21] and represents a compromise between accuracy and computational efficiency. The nonbonded energy of the systems was relaxed by performing 1500 steps of steepest-descent energy minimization in the following way: for the first 1000 steps only the water molecules were allowed to move, in order to relax the H_2O–H_2O and complex–H_2O nonbonded interaction energy and to let the water molecules reorient in the electric field of the complex. The whole system was then relaxed for the last 500 steps, of which the first 100 were performed while constraining the atoms of the complexes to their initial coordinates. In order to achieve electrical neutrality, six sodium ions were included in the system as follows: the electrostatic interaction energy was calculated at all water oxygen positions, and the water molecule with the most positive interaction potential was replaced by a sodium ion. Subsequently, and before introducing the next ion, the water molecules were subjected to 50 steps of steepest-descent energy minimization to allow for the optimization of the Na^+–H_2O interactions. By following this procedure, the sodium ions were placed in a minimum-energy configuration around the DNA: echinomycin complexes, which favored equilibration of the systems. This method is similar to that used by van Gunsteren et al. for ion placement,[21] except for the intermediate minimization steps. After including the sodium ions, the systems were energy-minimized and subjected to molecular dynamics simulations in which both temperature and pressure were weakly coupled to thermal and pressure baths[52] with relaxation times of 0.1 and 0.6 ps, respectively. In a 3-ps heating phase, the temperature was raised to 300 K in steps of 10 K over 0.1-ps blocks, the velocities being reassigned according to a Maxwell-Boltzmann distribution at each new temperature. This was followed by an equilibration phase of 17 ps at 300 K in which the velocities were reassigned in the same way every 0.2 ps during the first 5 ps. The systems appeared to be equilibrated after this time (Figure 4), and the simulations were allowed to continue for 20 more ps at the same temperature, during which system coordinates were saved every 0.1 ps. The reference pressure was 1 atm throughout the simulations. The time step used was 1 fs in the heating period and 2 fs during the rest of the simulations. All bonds involving hydrogens were constrained to their equilibrium values by means of the SHAKE algorithm,[53] and the lists of nonbonded pairs were updated every 25 steps.

(5) Analysis of the Dynamics Trajectories. The intramolecular and intermolecular energies of the DNA:echinomycin complexes were monitored and analyzed using the 100 coordinate sets saved during the last 10 ps of the unrestrained simulations in water. This method was justified by the fact that during the simulations neither the drug nor the DNA underwent large conformational rearrangements leading to significant changes in the potential energy of the complexes (Figure 4 and discussion below). All of the energy analyses were performed using a cutoff of 8 Å and a dielectric constant of 1 for the nonbonded interactions. The conformation and helical parameters of the DNA tetramers were monitored by writing an interface to the helix analysis program NEWHEL92.[54] Additional programs for analyzing the torsional angles in the echinomycin molecule and distances and angles between echinomycin and DNA atoms during the 30–40-ps period of the simulations were written in FORTRAN-77 by J.G.

(6) Solvation Free Energies. The electrostatic term of the solvation free energies was calculated by a linearized Poisson–Boltzmann method,[55] as implemented in the DelPhi module of INSIGHT-II. Accessible surface areas were calculated with a spherical probe of 1.4-Å radius representing a water molecule, according to the method of Lee and Richards.[56] A dielectric of 2 was used for the DNA:echinomycin complexes, and the ion radius for the Stern layers was 2 Å. The solvation energies were obtained by performing calculations in vacuo ($\epsilon = 1$) and in aqueous solution ($\epsilon = 80$, $I = 0.145$ M), and the focusing method for the dielectric boundary conditions[57] was employed. The point charges and van der Waals radii assigned to the echinomycin and DNA atoms were those used in the molecular mechanics force field. In order to estimate the solvation contribution to the free energy of echinomycin binding to the DNA tetramers, the solvation energies of both the unbound DNA tetranucleotides and the echinomycin molecule were also calculated. The structures were obtained by performing molecular dynamics simulations covering a time span of 40 ps under the same conditions as for the DNA:echinomycin complexes. The solvent was also considered explicitly, periodic boundary conditions were applied, and sodium counterions were included in the DNA solution boxes following the method outlined above. The initial structures were standard B-DNA[58] for the tetranucleotides and the intercalated conformation for the echinomycin molecule, which was found to be in agreement with the solution structure.[8,15,16]

Supplementary Material Available: Six tables containing covalent parameters (I) and charges (II) for echinomycin, lists of NOE distance constraints (III), lists of violations of NOE distances in the A(h) and T(w) complexes averaged over the 30–40-ps period of the unrestrained simulations in water (IV), averaged sugar–phosphate backbone, glycosyl dihedral angles, and pseudorotation phase angles in the A(h) and T(w) complexes (V), and averaged torsional angles of echinomycin in A(h) and T(w) (VI) (7 pages). Ordering information is given on any current masthead page.

Acknowledgment. We thank Dr. Xiaolian Gao and Professor Richard E. Dickerson for helpful comments, Dr. Chris Reynolds for his program to compute point charges, and Biosym Technologies, Inc., for a license to use their graphics programs. This research has been financed in part by the Spanish Comisión Interministerial de Ciencia y Tecnología (FAR91-0277) and the University of Alcalá de Henares (Madrid, Spain). J.G. is recipient of a predoctoral grant from the Spanish Ministerio de Educación y Ciencia.

References

(1) For a review, see: *Molecular Basis of Specificity in Nucleic Acid-Drug Interactions*; Pullman, B., Jortner, J., Eds.; Kluwer Academic Publishers: Dordrecht, 1990.
(2) Lee, J. S.; Waring, M. J. Interaction between Synthetic Analogues of Quinoxaline Antibiotics and Nucleic Acids. *Biochem. J.* **1978**, *173*, 129–144.
(3) Gago, F.; Richards, W. G. Netropsin Binding to Poly[d(IC)]·poly[d(IC)] and Poly[d(GC)]·poly[d(GC)]: A Computer Simulation. *Mol. Pharmacol.* **1990**, *37*, 341–346.
(4) Reviewed in Waring, M. J. The Molecular Basis of Specific Recognition Between Echinomycin and DNA. In ref 1, pp 225–245.
(5) Muss, H. B.; Blessing, J. A.; Eddy, G. L.; McGehee, R. Echinomycin (NSC 526417) in Recurrent and Metastatic Squamous Cell Carcinoma of the Cervix. A phase II Trial of the Gynecologic Oncology Group. *Invest. New Drugs* **1992**, *10*, 25–26.
(6) Low, C. M. L.; Drew, H. R.; Waring, M. J. Sequence-specific Binding of Echinomycin to DNA: Evidence for Conformational Changes Affecting Flanking Sequences. *Nucleic Acids Res.* **1984**, *12*, 4865–4879.
(7) Van Dyke, M. M.; Dervan, P. B. Echinomycin Binding Sites in DNA. *Science* **1984**, *225*, 1122–1127.
(8) Ughetto, G.; Wang, A. H.-J.; Quigley, G. J.; van der Marel, G. A.; van Boom, J. H.; Rich, A. A Comparison of the Structure of Echinomycin and Triostin A Complexed to a DNA Fragment. *Nucleic Acids Res.* **1985**, *13*, 2305–2323.
(9) Wang, A. H.-J.; Ughetto, G.; Quigley, G. J.; Hakoshima, T.; van der Marel, G. A.; van Boom, J. H.; Rich, A. The Molecular Structure of a DNA-triostin A Complex. *Science* **1984**, *225*, 1115–1121.
(10) Wang, A. H.-J.; Ughetto, G.; Quigley, G. J.; Rich, A. Interactions of Quinoxaline Antibiotic and DNA: The Molecular Structure of a Triostin A-d(GCGTACGC) Complex. *J. Biomol. Struct. Dyn.* **1986**, *4*, 319–342.
(11) Gao, X.; Patel, D. J. NMR Studies of Echinomycin Bisintercalation Complexes with d(A1-C2-G3-T4) and d(T1-C2-G3-A4) Duplexes in Aqueous Solution: Sequence-Dependent Formation of Hoogsteen A1·T4 and Watson–Crick T1·A4 Base Pairs Flanking the Bisintercalation Site. *Biochemistry* **1988**, *27*, 1744–1751.

(12) Gao, X.; Patel, D. J. Antitumour Drug-DNA Interactions: NMR Studies of Echinomycin and Chromomycin Complexes. *Q. Rev. Biophys.* **1989**, *22*, 93–138.
(13) Gilbert, D. E.; Feigon, J. The DNA Sequence at Echinomycin Binding Sites Determines the Structural Changes Induced by Drug Binding: NMR Studies of Echinomycin Binding to [d(ACGTACGT)]$_2$ and [d(TCGATCGA)]$_2$. *Biochemistry* **1991**, *30*, 2483–2494.
(14) Gilbert, D. E.; Feigon, J. Proton NMR Studies of the [d(ACGTATACGT)]$_2$-2echinomycin Complex: Conformational Changes between Echinomycin Binding Sites. *Nucleic Acids Res.* **1992**, *20*, 2411–2420.
(15) Cheung, H. T.; Feeney, J.; Roberts, G. C. K.; Williams, D. H.; Ughetto, G.; Waring, M. J. The Conformation of Echinomycin in Solution. *J. Am. Chem. Soc.* **1978**, *100*, 46–54.
(16) Williamson, M. P.; Williams, D. H. Manipulation of the Nuclear Overhauser Effect by the Use of a Viscous Solvent: the Solution Conformation of the Antibiotic Echinomycin. *J. Chem. Soc., Chem. Commun.* **1981**, 165–166.
(17) Alfredson, T. V.; Maki, A. H.; Waring, M. J. Optically Detected Triplet-State Magnetic Resonance Studies of the DNA Complexes of the Bisquinoline Analogue of Echinomycin. *Biochemistry* **1991**, *30*, 9665–9675.
(18) Part of this work has been presented in poster form: Gallego, J.; Gago, F. Hoogsteen versus Watson–Crick Base-pairing in Echinomycin-DNA Complexes. XIIth International Symposium on Medicinal Chemistry, Basel, 1992.
(19) Singh, U. C.; Pattabiraman, N.; Langridge, R.; Kollman, P. A. Molecular Mechanical Studies of d(CGTACG)$_2$: Complex of Triostin A with the Middle AT Base Pairs in either a Hoogsteen or Watson–Crick Pairing. *Proc. Natl. Acad. Sci. U.S.A.* **1986**, *83*, 6402–6406.
(20) Impey, R. W.; Madden, P. A.; Mc Donald, I. R. Hydration and Mobility of Ions in Solution. *J. Phys. Chem.* **1983**, *87*, 5071–5083.
(21) Van Gunsteren, W. F.; Berendsen, H. J. C.; Geurtsen, R. G.; Zwinderman, H. R. J. A Molecular Computer Dynamics Simulation of an Eight-Base-Pair DNA Fragment in Aqueous Solution: Comparison with Experimental Two-Dimensional NMR Data. *Ann. N. Y. Acad. Sci.* **1986**, *482*, 287–303.
(22) Gao, X. Personal communication.
(23) Gavezzotti, A. The calculation of Molecular Volumes and the Use of Volume Analysis in the Investigation of Structure Media and Solid-State Organic Reactivity. *J. Am. Chem. Soc.* **1983**, *105*, 5220–5225.
(24) Connolly, M. L. Molecular Surface; *QCPE 429*, Quantum Chemistry Program Exchange, Indiana University, Bloomington, IN 47405.
(25) Wakelin, L. P. G.; Waring, M. J. The Binding of Echinomycin to Deoxyribonucleic Acid. *Biochem. J.* **1976**, *157*, 721–740.
(26) Kalman, J. R.; Blake, T. J.; Williams, D. H.; Feeney, J.; Roberts, G. C. K. The Conformations of Triostin A in Solution. *J. Chem. Soc., Perkin Trans. 1* **1979**, 1313–1321.
(27) Sheldrick, G. M.; Guy, J. J.; Kennard, O.; Rivera, V.; Waring, M. J. Crystal and Molecular Structure of the DNA-binding Antitumour Antibiotic Triostin A. *J. Chem. Soc., Perkin Trans. 2* **1984**, 1601–1605.
(28) Alfredson, T. V.; Maki, A. H. Phosphorescence and Optically Detected Magnetic Resonance Studies of Echinomycin-DNA Complexes. *Biochemistry* **1990**, *29*, 9052–9064.
(29) Gago, F.; Reynolds, C.; Richards, W. G. The Binding of Nonintercalative Drugs to Alternanting DNA Sequences. *Mol. Pharmacol.* **1989**, *35*, 232–241.
(30) Rein, R. Studies of Biomolecular Interactions: Principles of Nucleic Acid Structure and Function from the Point of View of Constituent Interactions. In *Perspectives in Quantum Chemistry and Biochemistry*; Pullman, B., Ed.; John Wiley & Sons: New York, 1978; Vol. II, pp 307–362.
(31) Weiner, S. J.; Kollman, P. A.; Nguyen, D. T.; Case, D. A. An All Atom Force Field for Simulations of Proteins and Nucleic Acids. *J. Comput. Chem.* **1986**, *7*, 230–252.
(32) Stewart, J. J. P. MOPAC, version 6.0; *QCPE 455*, Quantum Chemistry Program Exchange, Indiana University, Bloomington, IN 47405.
(33) (a) *Tables of Experimental Dipole Moments*; McClellan, A. L., Ed.; Rahara Enterprises: El Cerrito, 1974; Vol. II. (b) *Ibid.* 1989; Vol. III.
(34) Low, L. C. M.; Olsen, R. K.; Waring, M. J. Sequence Preferences in the Binding to DNA of Triostin A and TANDEM as Reported by DNase I Footprinting. *FEBS Lett.* **1984**, *176*, 414–420.
(35) Addess, K. J.; Gilbert, D. E.; Olsen, R. K.; Feigon, J. Proton NMR Studies of [N-MeCys^3,N-MeCys^7]TANDEM Binding to DNA Oligonucleotides: Sequence-Specific Binding at the TpA Site. *Biochemistry* **1992**, *31*, 339–350.
(36) Fox, K. R.; Gauvreau, D.; Goodwin, D. C.; Waring, M. J. Binding of Quinoline Analogues of Echinomycin to Deoxyribonucleic Acid. Role of the Chromophores. *Biochem. J.* **1980**, *191*, 729–742.
(37) Low, C. M. L.; Fox, K. R.; Waring, M. J. DNA Sequence-selectivity of Three Biosynthetic Analogues of the Quinoxaline Antiobiotics. *Anti-Cancer Drug Design* **1986**, *1*, 149–160.
(38) Searle, M. S.; Wickham, G. Hoogsteen versus Watson–Crick A-T Base-pairing in DNA Complexes of a New Group of 'Quinomycin-like' Antibiotics. *FEBS Lett.* **1990**, *272*, 171–174.
(39) Mendel, D.; Dervan, P. B. Hoogsteen Base Pairs Proximal and Distal to Echinomycin Binding Sites on DNA. *Proc. Natl. Acad. Sci. U.S.A.* **1987**, *84*, 910–914.
(40) Portugal, J.; Fox, K. R.; McLean, M. J.; Richenberg, J. L.; Waring, M. J. Diethyl Pyrocarbonate can Detect a Modified DNA Structure Induced by the Binding of Quinoxaline Antibiotics. *Nucleic Acids Res.* **1988**, *16*, 3655–3670.
(41) McLean, J. M.; Seela, F.; Waring, M. J. Echinomycin-induced Hypersensitivity to Osmium Tetroxide of DNA Fragments Incapable of Forming Hoogsteen Base Pairs. *Proc. Natl. Acad. Sci. U.S.A.* **1989**, *86*, 9687–9691.
(42) (a) Seibel, G.; Singh, U. C.; Weiner, S. J.; Caldwell, J.; Kollman, P. A. *AMBER (UCSF)*: *Assisted Model Building with Energy Refinement*, version 3.0, Revision A, 1989. (b) Pearlman, D. A.; Case, D. A.; Caldwell, J.; Seibel, G.; Singh, U. C.; Weiner, P.; Kollman, P. A. *AMBER* version 4.0, 1991. Department of Pharmaceutical Chemistry, University of California, San Francisco.
(43) INSIGHT-II, version 2.1.0; Biosym Technologies, 9685 Scranton Road, San Diego, CA 92121-2777.
(44) Jorgensen, W. L.; Chandrasekhar, J.; Madura, J. D. Comparison of Simple Potential Functions for Simulating Liquid Water. *J. Chem. Phys.* **1983**, *79*, 926–935.
(45) Aqvist, J. Ion-Water Interaction Potentials Derived from Free Energy Perturbation Simulations. *J. Phys. Chem.* **1990**, *94*, 8021–8024.
(46) Weiner, S. J.; Kollman, P. A.; Case, D. A.; Singh, U. C.; Ghio, C.; Alagona, G.; Profeta, S.; Weiner, P. A New Force Field for Molecular Mechanical Simulation of Nucleic Acids and Proteins. *J. Am. Chem. Soc.* **1984**, *106*, 765–784.
(47) Hopfinger, A. J.; Pearlstein, R. A. Molecular Mechanics Force-Field Parameterization Procedures. *J. Comput. Chem.* **1984**, *5*, 486–499.
(48) Ferenczy, G. G.; Reynolds, C. A.; Richards, W. G. Semiempirical AM1 Electrostatic Potentials and AM1 Electrostatic Potential Derived Charges: A Comparison with ab initio Values. *J. Comput. Chem.* **1990**, *11*, 159–169.
(49) Orozco, M.; Laughton, C. A.; Herzyk, P.; Neidle, S. Molecular-Mechanics Modelling of Drug-DNA Structures: the Effects of Differing Dielectric Treatment on Helix Parameters and Comparison with a Fully Solvated Structural Model. *J. Biomol. Struct. Dyn.* **1990**, *8*, 359–373.
(50) Gronenborn, A. M.; Clore, G. M. Analysis of the Relative Contributions of the Nuclear Overhauser Interproton Distance Restraints and the Empirical Energy Function in the Calculation of Oligonucleotide Structures Using Restrained Molecular Dynamics. *Biochemistry* **1989**, *28*, 5978–5984.
(51) Wang, A. H.-J.; Ughetto, G.; Quigley, G. J.; Rich, A. Interactions between an Anthracycline Antibiotic and DNA: Molecular Structure of Daunomycin Complexed to d(CpGpTpApCpG) at 1.2 Å Resolution. *Biochemistry* **1987**, *26*, 1152–1163.
(52) Berendsen, H. J. C.; Postma, J. P. M.; van Gunsteren, W. F.; DiNola, A.; Haak, J. R. Molecular Dynamics with Coupling to an External Bath. *J. Chem. Phys.* **1984**, *81*, 3684–3690.
(53) Ryckaert, J. P.; Ciccotti, G.; Berendsen, H. J. C. Numerical Integration of the Cartesian Equations of Motion of a System with Constraints: Molecular Dynamics of n-alkanes. *J. Comput. Phys.* **1977**, *23*, 327–341.
(54) Dickerson, R. E. NEWHEL92. *Brookhaven Protein Data Bank*, 1992.
(55) Gilson, M. K.; Honig, B. Calculation of the Total Electrostatic Energy of a Macromolecular System: Solvation Energies, Binding Energies, and Conformational Analysis. *Proteins* **1988**, *4*, 7–18.
(56) Lee, B.; Richards, F. M. The Interpretation of Protein Structure: Estimation of Static Accessibility. *J. Mol. Biol.* **1971**, *55*, 379–400.
(57) Gilson, M. K.; Sharp, K. A.; Honig, B. H. Calculating the Electrostatic Potential of Molecules in Solution: Method and Error Assessment. *J. Comput. Chem.* **1988**, *9*, 327–335.
(58) Arnott, S.; Hukins, D. W. L. Optimized parameters for A-DNA and B-DNA. *Biochem. Biophys. Res. Commun.* **1972**, *47*, 1504–1510.